Avalanche observations at the Ryggfonn test site, Norway, with correlation to snow and weather conditions

Peter Gauer* and Krister Kristensen

Norwegian Geotechnical Institute

Sognsveien 72, NO-0855 Oslo, Norway

ABSTRACT. The Norwegian Geotechnical Institute (NGI) has been running full-scale avalanche experiments at the Ryggfonn test-site in western Norway for close to 40 years. Data from this period involve observations from about 32 artificial avalanche releases and 158 natural ones. In this paper, we do an attempt to correlate avalanche observations and obtained measurements from the Ryggfonn path with snow and weather conditions at the time. In this way, we hope to obtain an improved data set useful for model calibration and to obtain information on avalanche release probability. The final aim is to contribute to the further improvement of the quality of hazard zoning.

Keywords: avalanche observations, weather conditions, avalanche probability, hazard zoning

1 INTRODUCTION

Hazard assessment in snow avalanche prone areas requires the knowledge of avalanche release probability and the specification of expected runout distances.

In the following, we attempt to correlate avalanche observations and obtained measurements from the Ryggfonn path with the snow and weather conditions at the time. In this way, we hope to obtain some information on the avalanche release probability and the influence of the snow conditions on avalanche dynamics.

2 DESCRIPTION OF THE RESEARCH SITE

NGI has been performing full-scale avalanche experiments at the Ryggfonn test-site in western Norway (61.96° N, 7.275° E) for 40 years. Figure 1 shows a map of the area.

The upper half of the north-facing track is a cirque with the main starting zone at the upper end. In addition, several minor release areas left and right of the main track also drain into the common runout area. The total vertical drop height is about 920 m and the horizontal runout distances typically range between 1500 and 1850 m with a maximum up to 2100 m. The mean slope angle of the main track is 29°. The track itself is slightly channeled. A more detailed description of the instrumentation can be found in (Gauer and Kristensen, 2013; Gauer et al., 2010a).

*Corresponding author's address:
Peter Gauer
Norwegian Geotechnical Institute,
P.O. Box 3930 Ullevål Stadion, NO–0806 Oslo, Norway
Tel: ++47 45 27 47 43; Fax: ++47 22 23 04 48; E-mail: pg@ngi.no

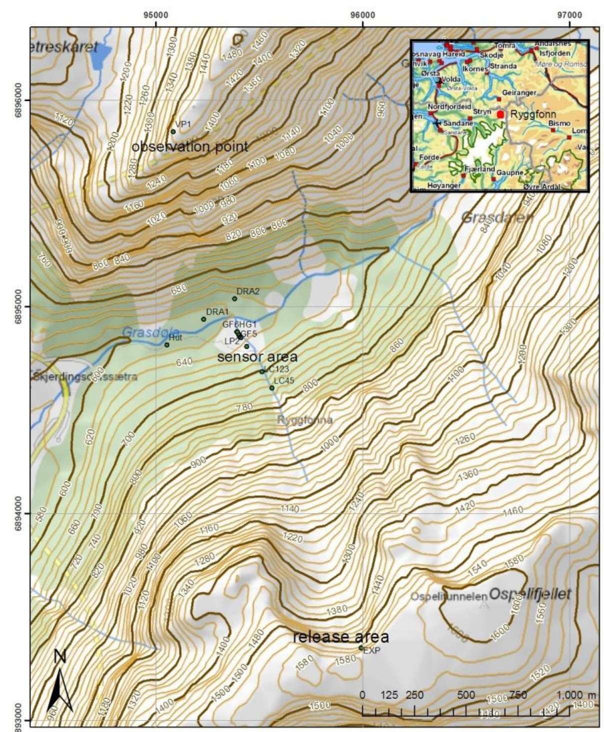

Figure 1: Map of the Ryggfonn test-site.

3 OBSERVATIONS AND MEASUREMENTS

3.1 Meteo data

The closest weather station to Ryggfonn is at the nearby snow research station Fonnbu (Jaedicke et al., 2008). Unfortunately, the weather records from Fonnbu are incomplete or lacking for parts of the considered period. Therefore, we use data derived from **seNorge** (Saloranta, 2012) as proxy in our study. The **seNorge** snow model operates with 1 × 1 km resolution, uses gridded observations of daily air temperature and precipitation as its input forcing, and simulates, among others, snow water equivalent (HSW), snow depth (HS). For our purpose, we use data corresponding to Fonnbu (model level ≈ 1087 m a.s.l.), to the release area of Ryggfonn (≈ 1600 m a.s.l.), and to the runout area (below 780 m a.s.l.). Here, we mainly focus on the data form the altitude of the release area. Unfortunately, we do not have sufficient snow temperature measurements from near the Ryggfonn path. Therefore, we use air temperature as an indicator for the snow conditions.

Although comparison between the available measurements from Fonnbu and the data from **seNorge** suggests a reasonable consistency, one has to keep the general difference between the two data sets in mind. The first one provides point measurements whereas **seNorge** provides spatial averages.

Figure 2 presents the relative frequency of the new snow water equivalent HNW_{1d} and HNW_{3d} at Ryggfonn, which are generally accepted as major parameters in avalanche forecasting.

3.2 Avalanche observations

In the period from winter 1973/1974 to winter 2012/2013, the avalanche data involve observations from about 32 artificial avalanche releases and 158 natural ones in the main path at Ryggfonn. This corresponds to an avalanche frequency of roughly four per year. A timeline of the events is given in Figure 3. As often, those observation are tainted with the uncertainty that due to the circumstances not all events were detected. Especially minor events, which did not run down to the valley bottom, might be missed. Another source of uncertainty is the exact timing of the observed avalanche events as some might be detected with a delay and therefore the mapping with the meteo-data might be slightly off.

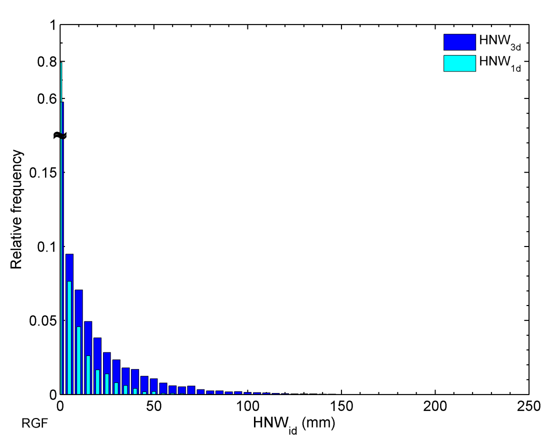

Figure 2: Relative frequency of the new snow water equivalent HNW_{1d} and HNW_{3d} at Ryggfonn.

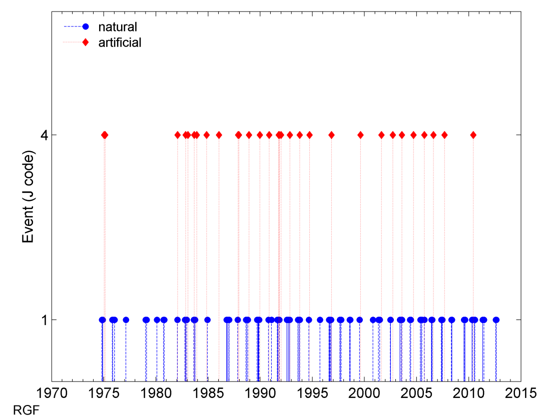

Figure 3: Timeline of the avalanche observations at Ryggfonn.

Figure 4 shows scatter plots of the one-day new snow water equivalent, HNW_{1d}, three-day-sum of the new snow water equivalent, HNW_{3d}, and daily air temperature, T, grouped as non-avalanche day, natural release and artificial release to give an impression of the prevailing conditions.

3.3 Avalanche probability

In avalanche hazard assessment, the probability of an avalanche in a given path is an important parameter. It is widely accepted that the new snow amount, especially the three-day-sum of new snow, is a major driving factor for natural avalanche occurrence (e.g. McClung and Schaerer, 2006). Besides its influence on the release probability, the amount of new snow is also linked to the probable fracture depth of the released snow slab in the avalanche starting zone and to the erodible mass along the track. The fracture depth is a typical input parameter that is required in modern avalanche models like **RAMMS** or **SamosAT** (Christen et al., 2010; Sampl and Granig, 2009).

Bakkehøi (1987) provided the cumulative probability distribution of the three-day precipitation previous to an avalanche at Raffelsteinfonn, an avalanche path in the proximity of the Ryggfonn path, and showed in addition the curve for a Gaussian normal cumulative distribution based on the same data (his Fig. 1). That is, Bakkehøi presented the conditional probability, $P(HNW_{3d}|A)$, of measuring HNW_{3d} at the day of an

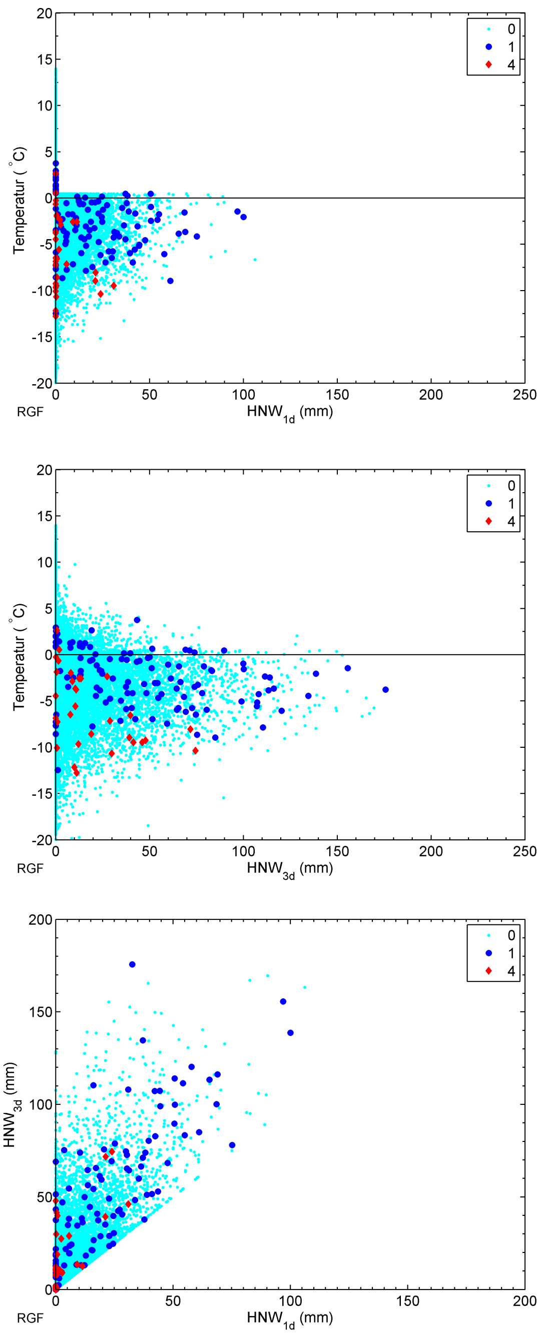

Figure 4: Scatter plot of the new snow water equivalent and daily air temperature during the observation period. 0 indicates no avalanche observation, 1 natural avalanche, and 4 artificial release.

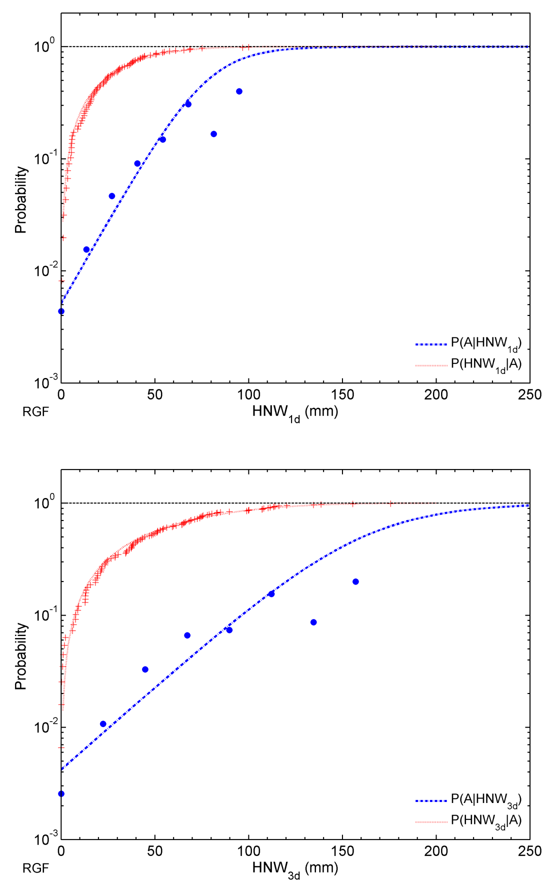

Figure 5: Cumulative probability distribution of the conditional probabilities $P(HNW_{id}|A)$ and $P(A|HNW_{id})$, where $i = 1, 3$. Here, (+) show single events whereas (•) indicate bin values.

avalanche event. This is different from the conditional probability, $P(A|HNW_{3d})$, of observing an avalanche given a measured HNW_{3d}. Meunier et al. (2005) presented an example for the conditional probability $P(A|HNW_{3d})$ for an avalanche path in the French Alps (their Fig 2. in section 6.2).

The difference of these two measures is shown in Figure 5 with regard to HNW_{1d} and HNW_{3d} for the Ryggfonn path. Here, the conditional probability is $P(HNW_{id}|A)$ is in both cases fitted to a generalized Pareto distribution whereas the conditional probability is $P(A|HNW_{id})$ is fitted using a logistic regression.

First of all, one has to emphasize that each of these probabilities are intrinsic to the path and its local conditions, like slope angle in the release zone or wind exposure. Second, both probabilities are important with respect to avalanche hazard zoning. $P(HNW_{id}|A)$ gives an indication of the fracture depth that could be expected and so provides information on an input parameter for avalanche models. On the other hand, $P(A|HNW_{id})$ combined with the probability, $P(HNW_{id})$, of observing HNW_{id} in a given period, provides information on the avalanche probability and so on the return period.

With respect to the probable fracture depths, the observed probability, $P(HNW_{3d}|A)$, shows similarities to calculations of the slab depth by Gaume et al. (2013).

3.4 Avalanche dynamics

Recently, Steinkogler et al. (2014) presented a detailed study on the influence of the snowpack conditions on the dynamics of five avalanches at the Vallée del la Sionne test site. Also Naaim and Durand (2012) tried to relate avalanche model parameters to niveo-meteorological parameters.

Here, we show only some preliminary observations from the Ryggfonn site. Figure 6 presents the influence of the daily air temperature on the averaged front velocity between the pylon (LC45) and the concrete wedge (LC123) in the sensor area (see Fig. 1). Although there is a considerable scatter, the figure suggests that

- U_{LC} decreases with increasing air temperature (—increased wetness of the snowpack—).

Figure 7 shows the influence of the amount of new snow, air temperature and air temperature gradient on the mean retarding acceleration (cf. Gauer, 2013). The mean retarding acceleration can also be considered as the ratio between fall height, H, and total travel distance, S, multiplied by the gravitational acceleration, g, (Gauer et al., 2010b):

$$|\bar{a}_{ret}| = \frac{g\,H}{S}\,. \qquad (1)$$

It can be regarded as a measure for the energy dissipation per unit mass during an avalanche descent. Higher retarding accelerations imply a lower avalanche mobility and so suggest shorter runout distances.

In general, the observations show a wide scatter. Nonetheless, some trends might be observed:

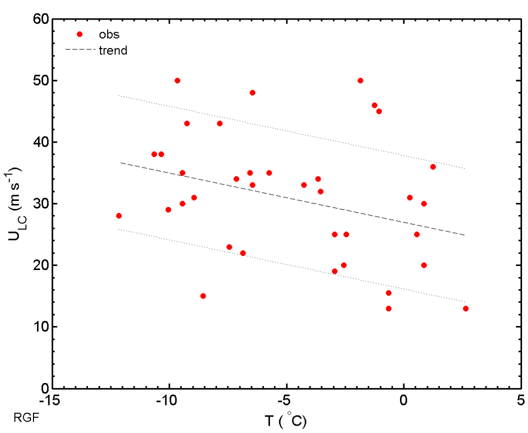

Figure 6: Influence of the air temperature on the front velocity between the pylon (LC45) and the concrete wedge (LC123).

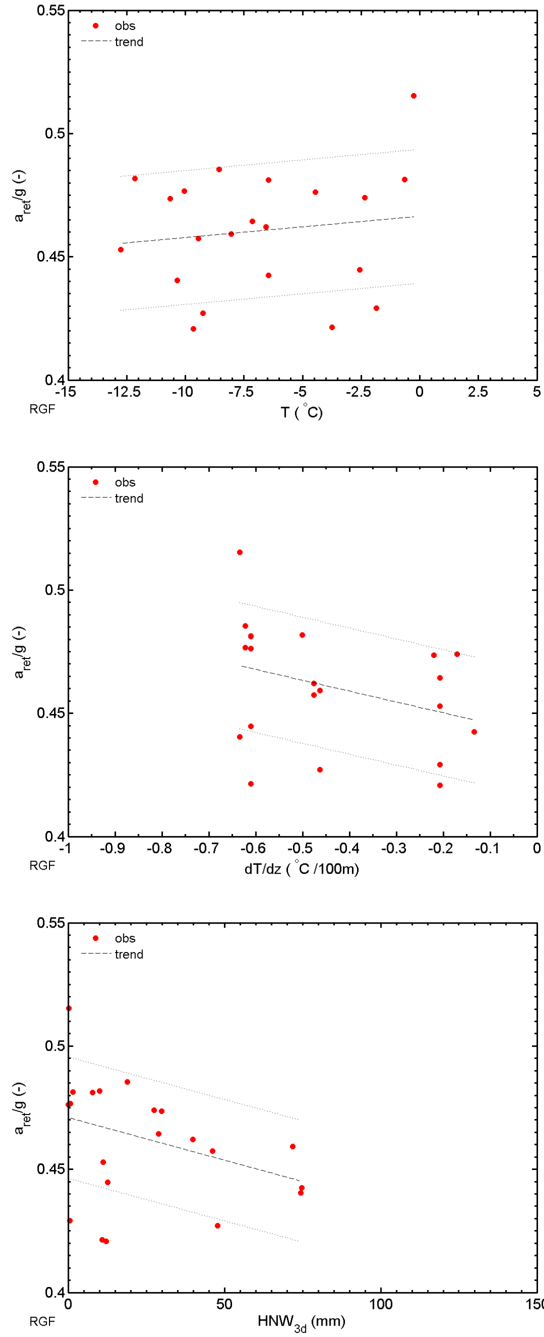

Figure 7: Influence of air temperature, air temperature gradient, and three-day-sum of the new snow water equivalent on the mean retarding acceleration.

- a_{ret} slightly increases with increasing air temperature;
- a_{ret} decreases with decreasing air temperature gradient (—more similar snow pack conditions along the track—);
- a_{ret} decreases with increasing amount of new snow.

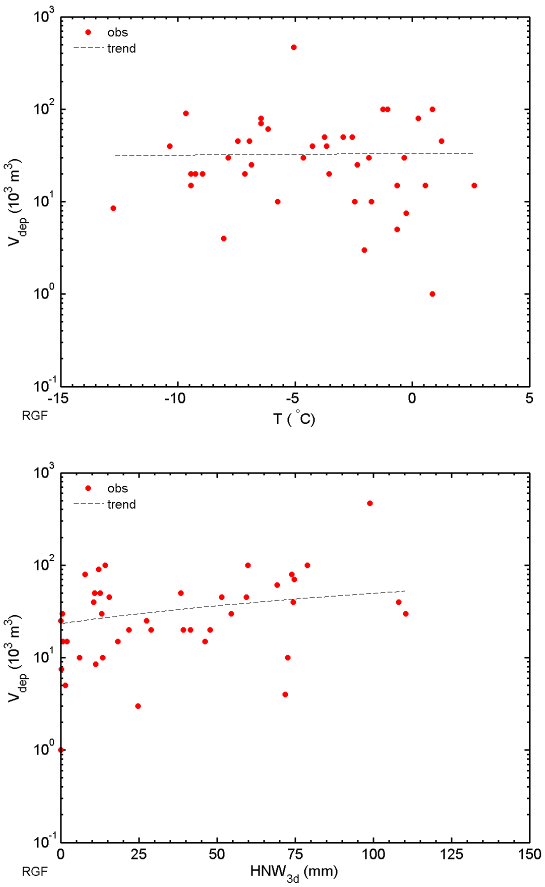

Figure 8: Influence of air temperature and three-day-sum of the new snow water equivalent on the estimated deposition volume in the runout zone.

Figure 8 depicts the influence of the amount of new snow and air temperature on the estimated deposition volume in the runout area. Seemingly,

- V_{dep} increases with increasing amount of new snow;
- no trend is obvious for the daily air temperature.

None of these trends seem really surprising and they are consistent with, e.g., the study by Steinkogler et al. (2014). More surprising might be the large scatter and that some of the trends are rather unincisive.

4 CONCLUSIONS

In this paper we present avalanche data from the Ryggfonn test site and correlate those observations with niveo-meteorological data. This preliminary study indicates some correlation that can help to improve the estimation of return periods and runout distances. Avalanche observations and measurements like the ones presented are still important to obtain sufficient data to improve our understanding on avalanche behavior and for model development and calibration. Here we see still potential for a further improvement of the quality of avalanche hazard zoning.

ACKNOWLEDGMENTS

Parts of this research was carried out through a snow avalanche research grant to NGI from the Ministry of Petroleum and Energy/Norwegian Water Resources and Energy Directorate.

REFERENCES

Bakkehøi, S., 1987: Snow avalanche prediction using a probabilistic method. *Avalanche Formation, Movement and Effects*, B. Salm and H.-U. Gubler, eds., Int. Assoc. Hydrol. Sci., Wallingford, Oxon OX10 8BB, UK, volume 162 of *IAHS Publ.*, 549–555.

Christen, M., J. Kowalski, and P. Bartelt, 2010: RAMMS: Numerical simulation of dense snow avalanches in three-dimensional terrain. *Cold Regions Science and Technology*, **63**, 1–14, doi:10.1016/j.coldregions.2010.04.005.

Gauer, P., 2013: Comparison of avalanche front velocity measurements: supplementary energy considerations. *Cold Regions Science and Technology*, **96**, 17–22, doi:10.1016/j.coldregions.2013.09.004.

Gauer, P., H. Breien, D. Issler, K. Kristensen, K. Kronholm, E. Lied, and K. Lied, 2010a: The upgraded full-scale avalanche test-site Ryggfonn, Norway. *Proceedings of the International Snow Science Workshop, Lake Tahoe, CA, October, 17–22, 2010*, 747–752.

Gauer, P. and K. Kristensen, 2013: 40 years of NGIs full-scale avalanche test-site Ryggfonn. *Proceedings of the International Snow Science Workshop. (ISSW) , Grenoble, October 7th - 11th 2013*.

Gauer, P., K. Kronholm, K. Lied, K. Kristensen, and S. Bakkehøi, 2010b: Can we learn more from the data underlying the statistical $\alpha - \beta$ model with respect to the dynamical behavior of avalanches? *Cold Regions Science and Technology*, **62**, 42–54, doi:10.1016/j.coldregions.2010.02.001.

Gaume, J., G. Chambon, N. Eckert, and M. Naaim, 2013: Influence of weak-layer heterogeneity on snow slab avalanche release: application to the evaluation of avalanche release depths. *Journal of Glaciology*, **59**, 423–437, doi:10.3189/2013JoG12J161.

Jaedicke, J., K. Kristensen, K. Lied, and S. Bakkeøi, 2008: Fonnbu, a new (old) platform for snow and avalanche research. *Proceedings Whistler 2008 International Snow Science Workshop September 21-27, 2008*, 598–603.

McClung, D. and P. Schaerer, 2006: *The Avalanche Handbook 3rd edition*. The Mountaineers Books, 1011 SW Klickitat Way, Seattle, Washington 98134.

Meunier, M., C. Ancey, and D. Richard, 2005: *Conceptual Approach to the Study of Snow Avalanches*. Update sciences & technologies Series.

Naaim, M. and Y. Durand, 2012: Dense avalanche friction coefficients. *Proceedings, 2012 International Snow Science Workshop, Anchorage, Alaska*.

Saloranta, T. M., 2012: Simulating snow maps for Norway: description and statistical evaluation of the seNorge snow model. *The Cryosphere*, **6**, 1323–1337, doi:10.5194/tc-6-1323-2012.

Sampl, P. and M. Granig, 2009: Avalanche simulation with SAMOS-AT. *Proceedings of the International Snow Science Workshop, Davos*, 519–523.

Steinkogler, W., B. Sovilla, and M. Lehning, 2014: Influence of snow cover properties on avalanche dynamics. *Cold Regions Science and Technology*, **97**, 121–131, doi:10.1016/j.coldregions.2013.10.002.